Electrochemical control of glucose oxidase-catalyzed redox reaction using an oil/water interface

Hotta, Hiroki
Sugihara, Takayasu
Osakai, Toshiyuki

(Citation)
Physical Chemistry Chemical Physics,6(13):3563-3568

(Issue Date)
2004-05-06

(Resource Type)
journal article

(Version)
Accepted Manuscript

(URL)
https://hdl.handle.net/20.500.14094/90000904

Electrochemical control of glucose oxidase-catalyzed redox reaction using an oil/water interface

Takayasu Sugihara, Hiroki Hotta, and Toshiyuki Osakai*

Department of Chemistry, Faculty of Science, Kobe University, Nada, Kobe 657-8501, Japan. Tel/Fax: 81 78 803 5682; E-mail: *osakai@kobe-u.ac.jp*

Glucose oxidase (GOD)-catalyzed electron transfers between some oxidants in nitrobenzene (NB) and glucose in water (W) were studied by cyclic voltammetry. When an electrically neutral compound, chloranil (CQ), was employed as the oxidant in NB, the enzymatic reaction could not be regulated because of the spontaneous transfer of CQ from NB to W. In this case, the voltammetric wave observed for the enzyme-catalyzed electron transfer was increased depending on the standing time until the voltage scan was started. However, when an ionic oxidant, dimethylferricenium ion ($DiMFc^+$), was employed as the oxidant, the

electrochemical control of the enzymatic reaction was achieved by controlling the interfacial transfer of $DiMFc^+$, so that well-reproducible voltammograms could be obtained for different concentrations of $DiMFc^+$ and for different scan rates. The voltammetric behaviors were successfully explained by a digital simulation based on the ion-transfer mechanism, which involves the interfacial transfer of $DiMFc^+$ and the succeeding GOD-catalyzed electron transfer which occurs not heterogeneously at the interface, but homogeneously in the W phase.

Introduction

Enzyme-catalyzed reactions in biomembranes are attractive for their specific catalyzing functions and significant roles *in vivo*. Respirative and photosynthetic electron transport chains, which are extremely efficient energy conversion systems, consist of sets of redox proteins located in biomembranes. A series of enzyme-catalyzed reactions control the direction of electron flow in a biomembrane and oxidative phosphorylation is driven by an electrochemical potential difference established across the biomembrane.[1] Thus, the electrochemical potential difference is considered to have an essentially important role in controlling enzyme-catalyzed reactions in biomembranes.

To investigate how the electrochemical potential difference affects the enzyme-catalyzed reactions, a polarized oil (O)/water (W) (or liquid/liquid) interface offers an intriguing and promising approach.[2,3] The electrochemical study of electron transfer reactions at the O/W interface as the simplest model of a

biomembrane would provide important keys for understanding electron transfer processes in biological systems. Kihara's group[4] studied the electron transfer between β-nicotinamide adenine dinucleotide (NADH) in W and some quinone derivatives in 1,2-dichloroethane (DCE). It was then reported that two different electron transfer processes occur depending on the potential difference across the interface. They also studied the electron transfer for flavin mononucleotide (FMN) at a DCE/W interface[5] and the electron transfer between L-ascorbic acid in W and 2,3,5,6-tetrachloro-1,4-benzoquinone (chloranil, CQ) in nitrobenzene.[6] The latter system has been studied in further detail by Osakai *et al.* using various electrochemical techniques.[7–11] On the other hand, however, there have been only a few electrochemical studies on electron transfers involving redox enzymes or proteins at the O/W interface. Williams *et al.*[12] first studied an enzyme-catalyzed electron transfer at a DCE/W interface by means of scanning electrochemical microscopy (SECM), in which glucose oxidase (GOD) mediated the electron transfer between β-D-glucose and dimethylferricenium ion ($DiMFc^+$) at the interface. Two different reaction mechanisms were proposed in which the enzyme-catalyzed electron transfer occurs heterogeneously at the O/W interface or homogeneously in the W phase, though the reaction mechanism remained to be clarified. Recently, Dryfe *et al.*[13] employed cyclic voltammetry as a *direct* method to study the electron transfer between cytochrome *c* and 1,1'-dimethylferrocene (DiMFc) at a DCE/W interface. These studies showed that such an electrochemical approach using the O/W interface is useful for studying electron

transfer reactions which involve redox proteins or enzymes.

In this study, we report direct voltammetric observations of GOD-catalyzed electron transfers between *β*-D-glucose in W and some oxidants in nitrobenzene (NB). When a neutral oxidant such as CQ was employed, the spontaneous electron transfer could not be regulated owing to an inevitable distribution of the oxidant into W. However, when an ionic oxidant ($DiMFc^+$) was employed, the enzyme-catalyzed electron transfer could be controlled voltammetrically by regulating the interfacial transfer of $DiMFc^+$. The reaction mechanism was studied in detail by the digital simulation analysis of cyclic voltammograms.

Experimental

Reagents

GOD (from Aspergillus niger) [EC 1.1.3.4] and *β*-D-glucose were purchased from Sigma and used as received. The concentration of GOD was determined spectrophotometrically using the absorption coefficient of 18 240 M^{-1} cm^{-1} at 460 nm.[14] The tetra-*n*-octylammonium salt of 12-tungstophosphate ($(TOcA)_3PW_{12}O_{40}$), which was used as the supporting electrolyte in NB, was prepared by equimolar addition of an ethanol solution of sodium tungstophosphate *n*-hydrate (Wako) and an ethanol solution of tetra-*n*-octylammonium bromide (Tokyo Kasei); the resulting crude salt was washed five times with deionized water and recrystallized from acetone. The dimethylferricenium salt of 12-tungstphosphate ($(DiMFc)_3PW_{12}O_{40}$) was prepared as follows: The 2.0 g of 1,1'-dimethylferrocene

(Tokyo Kasei) was dissolved in 30 ml of acetone, to which 1 ml of 30 % H_2O_2 and 1 ml of conc. HCl were added with heating and stirring. The resultant dimethylferricenium solution was then added to an equimolar aqueous–ethanol (1:1) solution of sodium tungstophosphate *n*-hydrate. The precipitate was purified by washing five times with *n*-hexane and deionized water, followed by drying at room temperature under reduced pressure. An aqueous solution of tetrapentylammonium chloride (TPnACl; Tokyo Kasei) was treated with silver chloride to remove iodide ion (a possible impurity); the concentration was determined by potentiometric titration with a standard silver nitrate solution. An analytical grade nitrobenzene (Wako) was treated before use with activated alumina for column chromatography (Wako; 200 mesh). All other reagents were of the highest grades available and were used as received.

Measurements

In cyclic voltammetry, the following electrochemical cell was used.

	I	II	III	IV	
Ag | AgCl	4 mM TPnACl 20 mM $MgSO_4$	*x* mM $(DiMFc)_3PW_{12}O_{40}$ 6.7 mM $(TOcA)_3PW_{12}O_{40}$	10 mM glucose 9.3 μM GOD 0.1 M LiCl	0.1 M LiCl	AgCl | Ag
(RE1)	(W)	(NB)	(W)	(W)	(RE2)

where RE1 and RE2 are the reference electrodes, and the double bar corresponds to the polarized NB/W interface (surface area: 0.052 cm^2). The pH of the aqueous phase (III) was adjusted to 7.0 with a 50 mM NaH_2PO_4–Na_2HPO_4 buffer. Two platinum coil electrodes were immersed into the respective phases and used as the

counter electrodes. The interface between phases I and II was formed in a Luggin capillary. Although the respective phases contained no common ion, the Galvani potential difference was found to be practically time-independent at least for several hours after preparation of the reference electrode. The reproducibility of the electrode potential was also very good (± 5 mV). The interface between phases III and IV was formed by means of a glass sinter. For further details of the electrolytic cell, see the previous paper.[15] Both the W and NB phases were deoxygenated with N_2 gas for at least 30 min prior to voltammetric measurements. The temperature of the electrolytic cell was kept at 25 ± 0.1 °C using a thermostatic water circulator.

The voltammetric measurements were performed using the previous computer assisted system.[15] The NB/W interface was polarized by using a four-electrode potentiostat (Hokuto Denko Co., HA1010mM1A). The solution resistance (*ca.* 3.5 kΩ) was compensated by means of a positive feedback circuit attached to the potentiostat. The Galvani potential difference, $\Delta_{\mathrm{O}}^{\mathrm{W}}\phi$ ($\equiv \phi^{\mathrm{W}} - \phi^{\mathrm{O}}$), was estimated by referring to the half-wave (*i.e.*, midpoint) potential of the transfer of tetramethylammonium (TMA^+) ion, which is given by

$$E_{1/2,\mathrm{j}}^{\mathrm{r}} = \Delta_{\mathrm{O}}^{\mathrm{W}}\phi_{\mathrm{j}}^{\circ} + \frac{RT}{F}\ln\frac{\gamma_{\mathrm{j}}^{\mathrm{O}}\sqrt{D_{\mathrm{j}}^{\mathrm{W}}}}{\gamma_{\mathrm{j}}^{\mathrm{W}}\sqrt{D_{\mathrm{j}}^{\mathrm{O}}}} + \Delta E_{\mathrm{ref}} \qquad (1)$$

Here, $\Delta_{\mathrm{O}}^{\mathrm{W}}\phi_{\mathrm{j}}^{\circ}$ is the standard ion-transfer potential of ion j (here, TMA^+ with $\Delta_{\mathrm{O}}^{\mathrm{W}}\phi_{\mathrm{j}}^{\circ}$ = +0.035 V [16]), $\gamma_{\mathrm{j}}^{\alpha}$ and D_{j}^{α} are its activity coefficient and diffusion coefficient in phase α (= O or W), respectively, ΔE_{ref} is the constant which is determined only

by the reference electrodes employed, and R, T, and F have their usual meanings. By assuming $\gamma_j^O / \gamma_j^W = 1$ and $D_j^W / D_j^O = 2$ (*i.e.*, the reciprocal ratio of the viscosities of water and NB), the value of ΔE_{ref} was estimated to be +0.336 V.

The numerical calculations for cyclic voltammograms were performed by a normal explicit finite difference digital simulation technique with an exponentially expanding space grid method.[11,17,18] A simulation program was written in Microsoft Visual C++ (ver. 6.0) and used for the manual curve-fitting analysis. For the detail of digital simulation of cyclic voltammograms with an O/W interface, see previous papers.[11,18]

Results

Cyclic voltammetry

In Fig. 1, curves (a) and (b) show the representative cyclic voltammograms for the transfer of $DiMFc^+$, respectively, in the presence and absence of GOD at the NB/W interface (note that the voltammograms were obtained in the absence of the substrate, glucose, in W). Since the blank voltammogram, which was obtained in either the presence (c) or absence (d) of GOD, had no current peak, the well-defined voltammetric wave having a pair of peaks should correspond to the reversible ion transfer (IT) of $DiMFc^+$ across the NB/W interface. The insensitivity of the voltammogram to the existence of GOD showed that the IT process for $DiMFc^+$ was hardly affected by GOD. The cathodic (negative-current) peak corresponds to the IT of $DiMFc^+$ from NB to W, and the anodic

(positive-current) peak corresponds to the back IT. The peak separations (ΔE_p) for different scan rates (v = 10, 20, 50, 100, 200 mV s^{-1}) were constant at about 60 mV, showing that the IT should be reversible and obey the Nernst equation:

$$\Delta_O^W\phi = \Delta_O^W\phi^\circ_{DiMFc^+} + \frac{RT}{F}\ln\frac{[DiMFc^+]_O}{[DiMFc^+]_W} \quad (2)$$

where $\Delta_O^W\phi^\circ_{DiMFc^+}$ is the standard IT potential of $DiMFc^+$, and $[DiMFc^+]_O$ and $[DiMFc^+]_W$ are the interfacial concentrations in O and W, respectively. Accordingly, the midpoint potential between the cathodic and anodic peaks can be regarded as the half-wave potential given by eqn. (1). Based on the same assumptions described above, $\Delta_O^W\phi^\circ_{DiMFc^+}$ was determined to be –0.146 V, which was used as an experimentally determined parameter in the digital simulation.

As shown in Fig. 1, the addition of GOD did not cause any changes both in the voltammograms for the IT of $DiMFc^+$ (curves (a) and (b)) and the blank voltammograms (curves (c) and (d)). Although GOD is known to adsorb at an air/water interface[19] and also suspected to adsorb at an O/W interface,[12] the present result seems to suggest that GOD does not adsorb at the NB/W interface, at least in the potential range shown in Fig. 1. In the higher potential range, however, GOD was still suspected to adsorb at the interface and have some influence on the voltammogram (see below). Unless noted otherwise, GOD was added to the W phase throughout the experiments.

In Fig. 2 are shown cyclic voltammograms obtained in the presence of 10 mM glucose (A) for different concentrations of $DiMFc^+$ and (B) for different scan rates.

As seen in the figure, the anodic peak was depressed or disappeared, probably due to the catalytic oxidation of glucose by GOD in the W phase. Because $DiMFc^+$ works as an electron acceptor in the GOD-catalyzed oxidation,[20] the $DiMFc^+$ transferred from NB to W in the first cathodic scan should be reduced irreversibly to DiMFc by the enzymatic reaction. It is also noteworthy that the cathodic peak potential shifted slightly toward more positive potential as the concentration of $DiMFc^+$ was decreased. Such a peak shift was also observed when the scan rate was decreased, conspicuously at a lower scan rate of 5 mV s^{-1} (see Fig. 3). This clearly shows that the transfer of $DiMFc^+$ from NB to W is facilitated by the enzymatic reaction in W.

Reaction Mechanism

The above cyclic voltammograms would suggest that the GOD-catalyzed reaction proceeds homogeneously in W. A proposed model for the GOD-catalyzed electron transfer at the NB/W interface is shown in Fig. 4. In the model, the IT of $DiMFc^+$ from NB to W corresponds to the cathodic current shown in Fig. 2. The $DiMFc^+$ transferred to the W phase should be reduced therein to DiMFc by the GOD-catalyzed reaction, and the resultant hydrophobic DiMFc subsequently diffuses back to NB. Since the interfacial transfer of the neutral DiMFc gives no current, the enzymatic irreversible reduction of $DiMFc^+$ to DiMFc in W should cause disappearance of the anodic current, which was clearly observed in the voltammograms recorded at lower scan rates (Fig. 2B). At a high scan rate (100

mV s^{-1}), however, a small anodic current was observed, which can be attributed to the back transfer of $DiMFc^+$ remaining unreacted in the W phase. The observed potential shift of the cathodic peak can be elucidated in terms of the facilitation effect of the enzymatic reaction on the transfer of $DiMFc^+$ from NB to W. Thus, the whole behavior of the cyclic voltammograms could be explained by the facilitated IT of $DiMFc^+$ by the homogeneous GOD-catalyzed electron transfer reaction. Therefore, we call the proposed reaction model "IT mechanism".

An alternative reaction model, which we call "electron-transfer (ET) mechanism", might be possible, in which a GOD-catalyzed ET occurs *heterogeneously* at the interface. This is indeed the case of our interest connected to the enzyme-catalyzed ET in biomembranes. However, the ET mechanism failed to explain the above experimental results. In the ET mechanism, the GOD which exists at the NB/W interface catalyzes the heterogeneous ET between glucose in W and $DiMFc^+$ in NB. Accordingly, the cathodic current may be explained by the heterogeneous ET at the interface, but the anodic current observed at a higher scan rate (curve (d) in Fig. 2B) cannot be explained because of the essential difficulty of the enzymatic backward reaction. Thus, the present GOD-catalyzed ET at the NB/W interface is considered to proceed primarily *via* the IT mechanism. Nevertheless, we would like to add that the present results cannot exclude entirely the possibility of the ET mechanism. The ET *via* the ET mechanism might be hidden behind that *via* the IT mechanism.

Digital simulation

For further confirmation of the validity of the IT mechanism, a digital simulation analysis of cyclic voltammograms was performed. In the simulation, it was assumed that the IT of $DiMFc^+$ at the NB/W interface is very fast and its potential-dependent distribution across the interface obeys the Nersnt equation (eqn. (2)). The partition of DiMFc at the interface was also assumed to be in equilibrium:

$$\frac{[\mathrm{DiMFc}]_\mathrm{O}}{[\mathrm{DiMFc}]_\mathrm{W}} = K_\mathrm{D}\ (\text{constant}) \tag{3}$$

where $[DiMFc]_O$ and $[DiMFc]_W$ are the interfacial concentrations of DiMFc in NB and in W, respectively. Though the K_D of DiMFc was failed to be obtained experimentally owing to the highly hydrophobic nature of DiMFc, the K_D for ferrocene (Fc) has been reported to be in the order of thousands.[18,21,22] Since DiMFc is considered to be more hydrophobic than Fc, the value of K_D for DiMFc was tentatively set as 1×10^4. The uncertainty of this parameter would give some errors in the calculation of the concentration profile of DiMFc, but hardly affected the simulation results for cyclic voltammograms. This is because the irreversible enzymatic reaction in W should not be affected by the concentration of DiMFc as the reaction product (see below). The diffusion coefficients of DiMFc, $DiMFc^+$, and glucose, used for the simulation, were determined or estimated as described below: The diffusion coefficient of $DiMFc^+$ in NB was determined to be 1.8×10^{-6} cm^2 s^{-1} by conventional cyclic voltammetry with a platinum electrode in NB, and the diffusion coefficient of DiMFc in NB was assumed to be identical to that

of $DiMFc^+$. The diffusion coefficients of $DiMFc^+$ and DiMFc in W were set as 3.6 $\times 10^{-6}$ cm^2 s^{-1}, on the assumption that $D^w/D^{NB} = 2$ (*i.e.*, the reciprocal of the viscosity ratio of water and NB).

The enzyme kinetics of GOD in W was treated in the same manner as the previous report.[14] The GOD reaction with oxygen as an electron acceptor is known to proceed in a ping-pong mechanism:

$$GOD_{ox} + \text{glucose} \rightleftharpoons \text{GOD-glucose} \rightarrow GOD_{red} + \text{gluconic acid} \quad (4)$$

$$GOD_{red} + O_2 \rightleftharpoons GOD\text{-}O_2 \rightarrow GOD_{ox} + H_2O_2 \quad (5)$$

where GOD-glucose and GOD-O_2 represent the corresponding enzyme-substrate complexes. The GOD reaction with an artificial one-electron acceptor (here, $DiMFc^+$) could be assumed to proceed in two steps:[14]

$$GOD_{red} + M_{ox} \rightleftharpoons GOD\text{-}M_{Ox} \rightarrow GOD_{sem} + M_{red} \quad (6)$$

$$GOD_{sem} + M_{ox} \overset{\text{fast}}{\rightarrow} GOD_{ox} + M_{red} \quad (7)$$

where M_{ox} and M_{red} correspond to $DiMFc^+$ and DiMFc, respectively. It is here assumed that the one-electron oxidation of GOD_{red} follows a simple ping-pong mechanism to yield its flavosemiquinone intermediate (GOD_{sem}) and that the succeeding one-electron oxidation of GOD_{sem} is not a rate-determining step. By applying the steady-state approximation method to reactions (4) and (6), one can obtain the following equation for the steady-state enzyme kinetics (v = –d[glucose]/dt) of the GOD reaction with $DiMFc^+$ in W:

$$v = \frac{V_{max}}{1 + \dfrac{K_{glucose}}{[\text{glucose}]} + \dfrac{K_{DiMFc^+}}{[DiMFc^+]_W}} \quad (8)$$

where V_{max} is the maximum velocity of the GOD reaction which is given by V_{max} = k_{cat}[GOD] (k_{cat} being the catalytic constant), and $K_{glucose}$ and K_{DiMFc^+} are Michaelis constants for glucose and $DiMFc^+$, respectively. From the overall stoichiometry of the GOD reaction, the velocity defined by eqn. (8) is written as:

$$v = -\frac{\mathrm{d[glucose]}}{\mathrm{d}t} = -\frac{1}{2} \times \frac{\mathrm{d[DiMFc]_W}}{\mathrm{d}t} = \frac{1}{2} \times \frac{\mathrm{d[DiMFc^+]_W}}{\mathrm{d}t} \quad (9)$$

In the simulation, the reported value of $K_{glucose}$ (= 29 mM[23]) was employed. Although this value might have some experimental error, the simulation results were not affected by changing the $K_{glucose}$ value in the range of 10 – 100 mM. This can be explained as follows: In the experimental conditions employed, the concentration of $DiMFc^+$ in W was in the micromolar order (see the concentration profile shown below), so that the concentration of glucose in excess (10 mM) could be assumed to be constant. Accordingly, the term $K_{glucose}$/[glucose] in eqn. (8) is usually constant and much smaller (thus, less significant) than the term K_{DiMFc^+}/[$DiMFc^+$].

Fig. 5 shows the simulation results for the cyclic voltammograms obtained under various measurement conditions. The cyclic voltammograms shown by solid lines in Panels (A), (B), (C), and (D) correspond to the baseline-corrected cyclic voltammograms for Figs. 1(a), 2A, 2B, and 3, respectively. As seen in the figure, the voltammograms obtained under any measurement conditions were successfully reproduced by using k_{cat} = 350 s^{-1} and K_{DiMFc^+} = 7 mM as the fitting parameters. These parameters were comparable with those reported in the

literature for ferrocenedicarboxylic acid (350 s^{-1} and 3.17 mM, respectively).[14] Note that these parameters were determined by manual curve fitting, *i.e.*, through trial and error, and were found to have uncertainties of ±50 s^{-1} for k_{cat} and ±2 mM for K_{DiMFc^+}. Thus, the IT mechanism was successfully used to explain the whole voltammetric behaviors of the GOD-catalyzed ET between glucose and $DiMFc^+$.

Additionally, it has been confirmed by the digital simulation that $DiMFc^+$ can certainly move into the W phase to react therein with GOD. Fig. 6 shows the snapshot of concentration profiles of $DiMFc^+$ and DiMFc, which was obtained by the simulation based on the IT mechanism, at $\Delta_O^W\phi$ = –0.18 V (*i.e.*, 15 s after a voltammetric sweep from –0.03 V at 10 mV s^{-1}). As seen in the figure, $DiMFc^+$ penetrates for *ca.* 100 μm into the W phase.

Discussion

In the present system, an electrochemical control of the enzymatic oxidation of glucose in the W phase was achieved by regulating the "supply" of the electron acceptor, *i.e.*, $DiMFc^+$. However, the ET reaction could not be controlled when a neutral compound was employed for the electron acceptor. Fig. 7 shows representative cyclic voltammograms which were obtained by using neutral CQ in place of $DiMFc^+$. Although a cathodic current spike was observed at around 0 V, which probably due to desorption of GOD from the interface, a pair of well-defined current peaks were observed in the lower potential region. This would be elucidated in terms of the GOD-catalyzed ET between glucose and CQ

in W, followed by an IT of the resultant semiquinone radical anion ($CQ^{\bullet-}$):

$$CQ\ (NB) \rightleftharpoons CQ\ (W) \tag{10}$$

$$Glucose + 2CQ \rightarrow gluconic\ acid + 2CQ^{\bullet-}\ (catalyzed\ by\ GOD\ in\ W) \tag{11}$$

$$CQ^{\bullet-}\ (W) \rightleftharpoons CQ^{\bullet-}\ (NB) \tag{12}$$

However, since the initial step (10), *i.e.*, the distribution of CQ to W, cannot be controlled by regulating the interfacial potential difference, the succeeding enzymatic reaction (11) would proceed spontaneously after formation of an O/W interface in the electrolytic cell. For this reason, the observed voltammetric wave due to the IT of $CQ^{\bullet-}$ (12) was increased depending on the standing time until the voltage scan was started (see Fig. 7). It should be noted that such a time-dependence of the voltammetric wave was not observed for the use of an ionic electron acceptor, $DiMFc^{+}$, because its IT could be controlled electrochemically.

In this study, we have successfully provided an electrochemical tool to study enzymatic reactions involving a hydrophobic reactant and their dependences on the Galvani potential difference across an O/W interface. This would be significant because enzymatic reactions in biomembranes commonly involve a lipophilic reactant and are considered to be under the influence of the membrane potential. In the present result, the heterogeneous ET at the O/W interface being catalyzed by a non-membrane enzyme (*i.e.*, GOD) was not observed. However, a plausible adsorption/desorption behavior of GOD at the O/W interface was demonstrated as shown in Fig. 7. Such an adsorption of an enzyme at the O/W

interface would possibly affect its enzymatic properties. It seems very interesting to study adsorption behaviors of membrane redox proteins like cytochrome *c* oxidase and their potential-dependent activities at O/W interfaces. Further studies are in progress.

Acknowledgements

We are grateful to Dr. Kenji Kano of Kyoto University for his helpful advice. This work was supported in part by Grant-in-Aids for Scientific Research from the Ministry of Education, Science, Sports and Culture of Japan.

References

1 P. Mitchell, *Science*, 1979, **206**, 1148.

2 A. G. Volkov, D. W. Deamer, D. L. Tanelian, V. S. Markin, *Liquid Interfaces in Chemistry and Biology*, Wiley, NewYork, 1998.

3 *Liquid Interfaces in Chemical, Biological, and Pharmaceutical Applications*, ed. A. G. Volkov, Marcel Dekker, Boca Raton, FL, 2001.

4 H. Ohde, K. Maeda, Y. Yoshida, S. Kihara, *Electrochim. Acta*, 1998, **44**, 23.

5 M. Suzuki, M. Matsui, S. Kihara, *J. Electroanal. Chem.*, 1997, **438**, 147.

6 M. Suzuki, S. Umetani, M. Matsui, S. Kihara, *J. Electroanal. Chem.*, 1997, **420**, 119.

7 T. Osakai, N. Akagi, H. Hotta, J. Ding, S. Sawada, *J. Electroanal. Chem.*, 2000, **490**, 85.

8 T. Osakai, H. Jensen, H. Nagatani, D. J. Fermín, H. H. Girault, *J. Electroanal. Chem.*, 2001, **510**, 43.

9 S. Sawada, M. Taguma, T. Kimoto, H. Hotta, T. Osakai, *Anal. Chem.*, 2002, **74**, 1177.

10 H. Hotta, N. Akagi, T. Sugihara, S. Ichikawa, T. Osakai, *Electrochem. Commun.*, 2002, **4**, 472.

11 T. Sugihara, H. Hotta, T. Osakai, *Bunseki Kagaku*, 2003, **52**, 665.

12 D. G. Georganopoulou, D. J. Caruana, J. Strutwolf, D. E. Williams, *Faraday Discuss.*, 2000, **116**, 109.

13 G. C. Lillie, S. M. Holmes, R. A. W. Dryfe, *J. Phys. Chem. B*, 2002, **106**, 12101.

14 R. Matsumoto, M. Mochizuki, K. Kano, T. Ikeda, *Anal. Chem.*, 2002, **74**, 3297.

15 S. Aoyagi, M. Matsudaira, T. Suzuki, H. Katano, S. Sawada, H. Hotta, S. Ichikawa, T. Sugihara, T. Osakai, *Electrochemistry*, 2002, **70**, 329.

16 J. Koryta, P. Vanysek, M. Brezina, *J. Electroanal. Chem.*, 1977, **75**, 211.

17 A. J. Bard, L. R. Faulkner, *Electrochemical Methods: Fundamentals and Applications*, Wiley, NewYork, 2001.

18 H. Hotta, S. Ichikawa, T. Sugihara, T. Osakai, *J. Phys. Chem. B*, 2003, **107**, 9717.

19 J. Rinuy, P. F. Brevet, H. H. Girault, *Biophys. J.*, 1999, **77**, 3350.

20 J. H. T. Luong, C. Masson, R. S. Brown, K. B. Male, A. L. Nguyen, *Biosens. Bioelectron.*, 1994, **9**, 577.

21 C. Wei, A. J. Bard, M. V. Mirkin, *J. Phys. Chem.*, 1995, **99**, 16033.

22 K. Nakatani, T. Uchida, H. Misawa, N. Kitamura, H. Masuhara, *J. Electroanal. Chem.*, 1994, **367**, 109.

23 P. N. Bartlett, K. F. E. Pratt, *J. Electroanal. Chem.*, 1995, **397**, 53.

Figure captions

Fig. 1 Cyclic voltammograms obtained in the absence of glucose: (a, b) 0.9 mM $DiMFc^+$ in NB in the presence (a) and absence (b) of 9.3 μM GOD in W; (c) 9.3 μM GOD in W in the absence of $DiMFc^+$; (d) neither $DiMFc^+$ nor GOD were dissolved in each phase. Scan rate: 10 mV s^{-1}.

Fig. 2 Cyclic voltammograms obtained in the presence of glucose: (A) for different concentrations of $DiMFc^+$: (a) 0.5 mM, (b) 0.9 mM, (c) 1.5 mM (scan rate: 20 mV s^{-1}); (B) for different scan rates: (a) 10 mV s^{-1}, (b) 20 mV s^{-1}, (c) 50 mV s^{-1}, (d) 100 mV s^{-1} ($[DiMFc^+]^*$ = 0.9 mM, [ ]* represents the bulk concentration).

Fig. 3 Cyclic voltammograms obtained at a lower scan rate (5 mV s^{-1}): (a) in the absence of glucose; (b) in the presence of glucose. Other experimental conditions are the same as in Fig. 2B.

Fig. 4 Proposed mechanism (IT mechanism) for the GOD-catalyzed oxidation of glucose by $DiMFc^+$.

Fig. 5 Regression results for the cyclic voltammograms obtained under various measurement conditions. The cyclic voltammograms shown by solid lines in Panels (A), (B), (C) and (D) correspond to the baseline-corrected cyclic

voltammograms for Figs. 1(a), 2A, 2B, and 3, respectively. Solid circles show the regression data.

Fig. 6 Snapshot of the concentration profiles of $DiMFc^+$ and DiMFc at $\Delta_O^W\phi = -0.18$ V, which were obtained by a digital simulation based on the IT mechanism. Initial conditions: [$DiMFc^+$]* = 0.9 mM, [glucose]* = 10 mM. Scan rate: 10 mV s^{-1}.

Fig. 7 Baseline-corrected cyclic voltammograms obtained by using CQ (20 mM in NB) as an electron acceptor in place of $DiMFc^+$. The W phase contained 10 mM glucose and 9.3 μM GOD. The voltammograms were recorded immediately after and every 5 min after the formation of a test interface, showing some increases in the cathodic and anodic peaks. Scan rate: 100 mV s^{-1}.

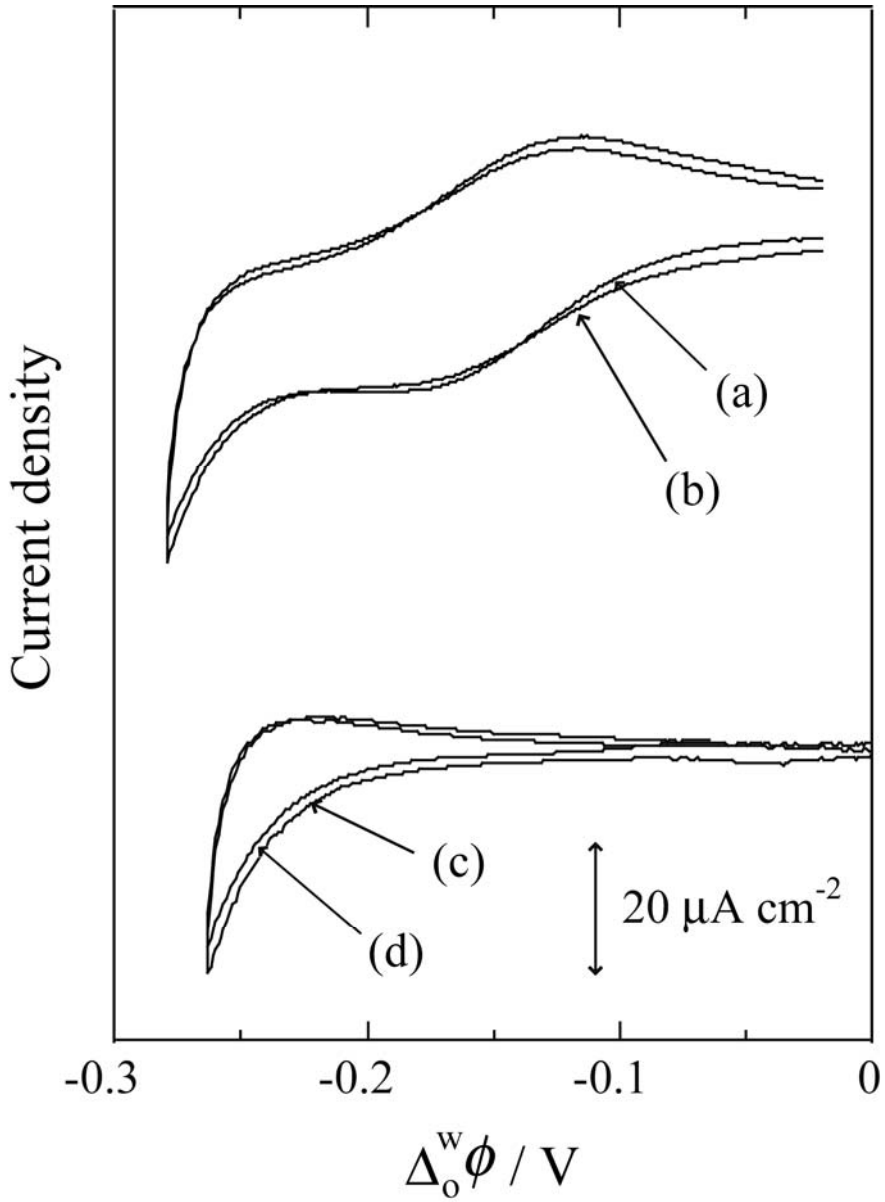

Fig. 1

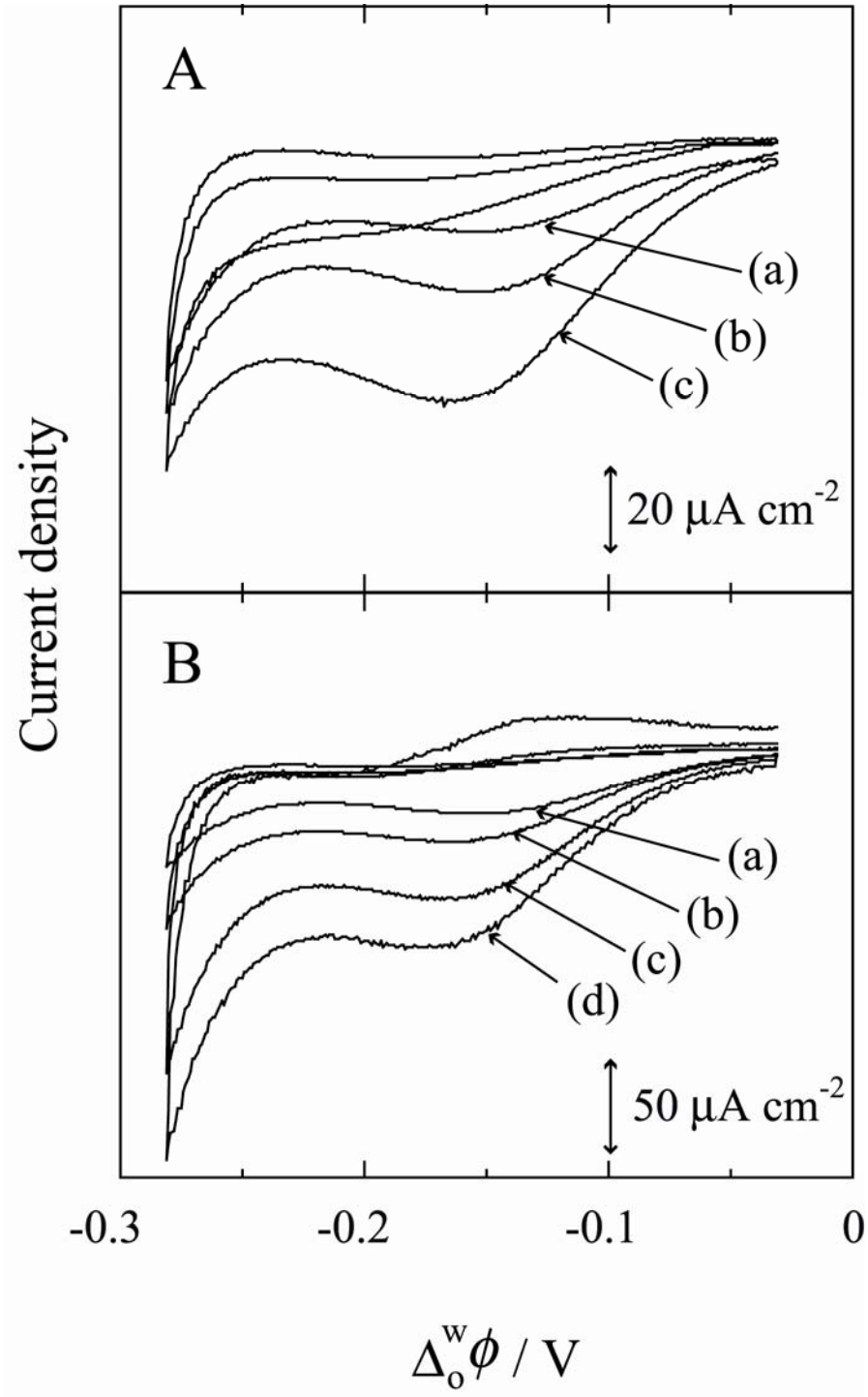

Fig. 2

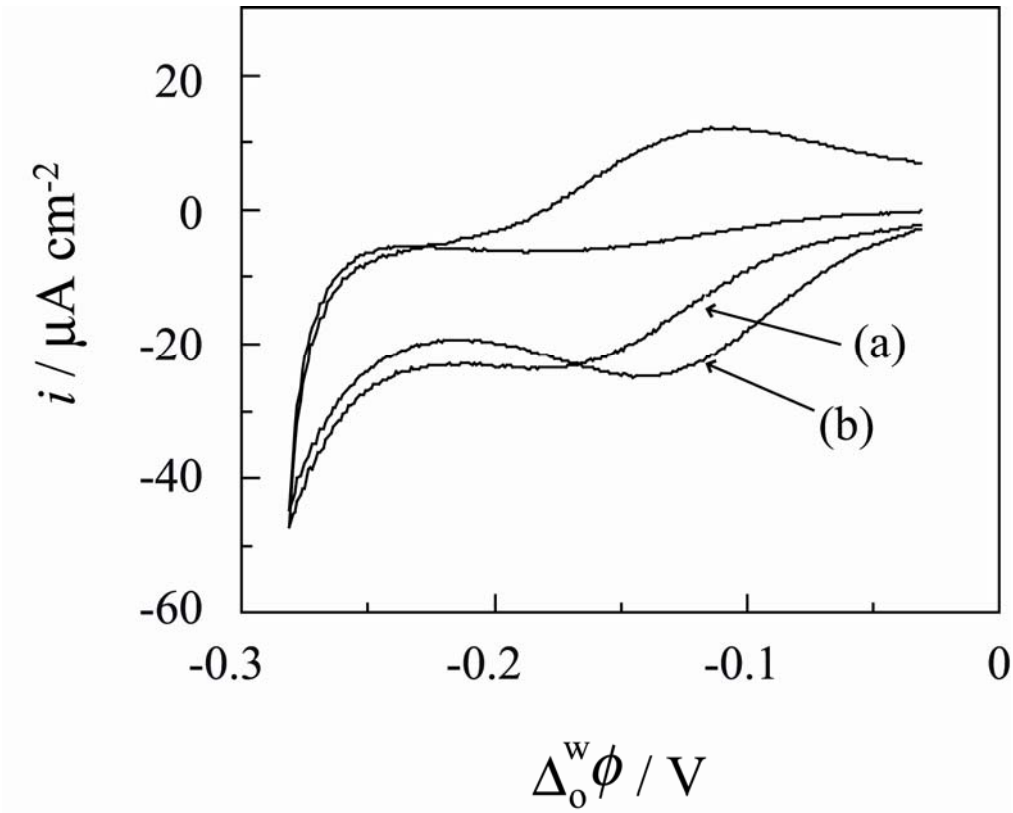

Fig. 3

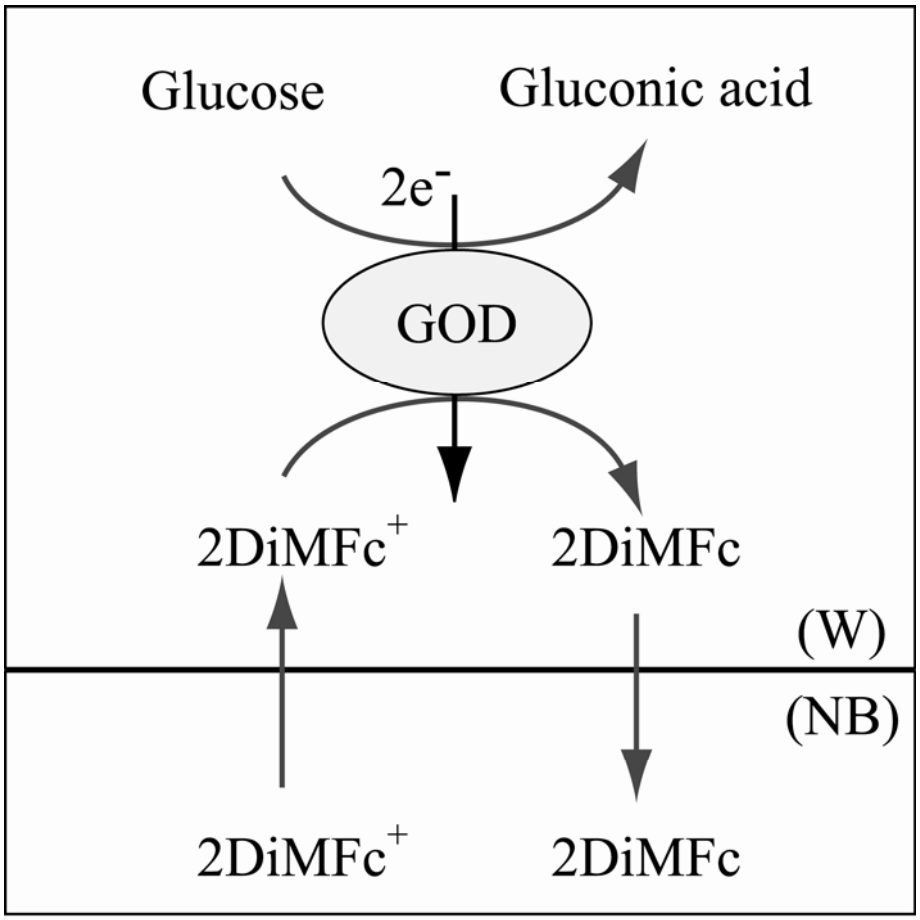
Glucose
Gluconic acid
2e-
GOD
2DiMFc+
2DiMFc
(W)
(NB)
2DiMFc+
2DiMFc

Fig. 4

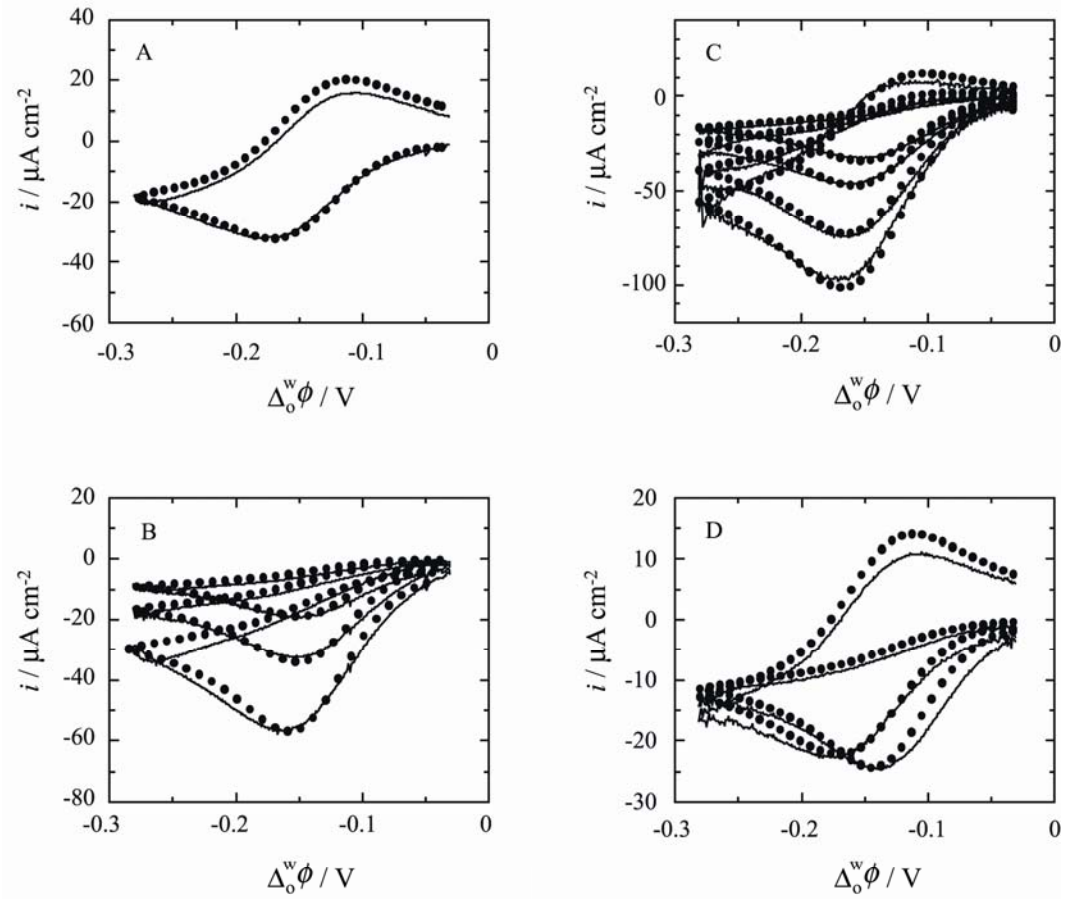

Fig. 5

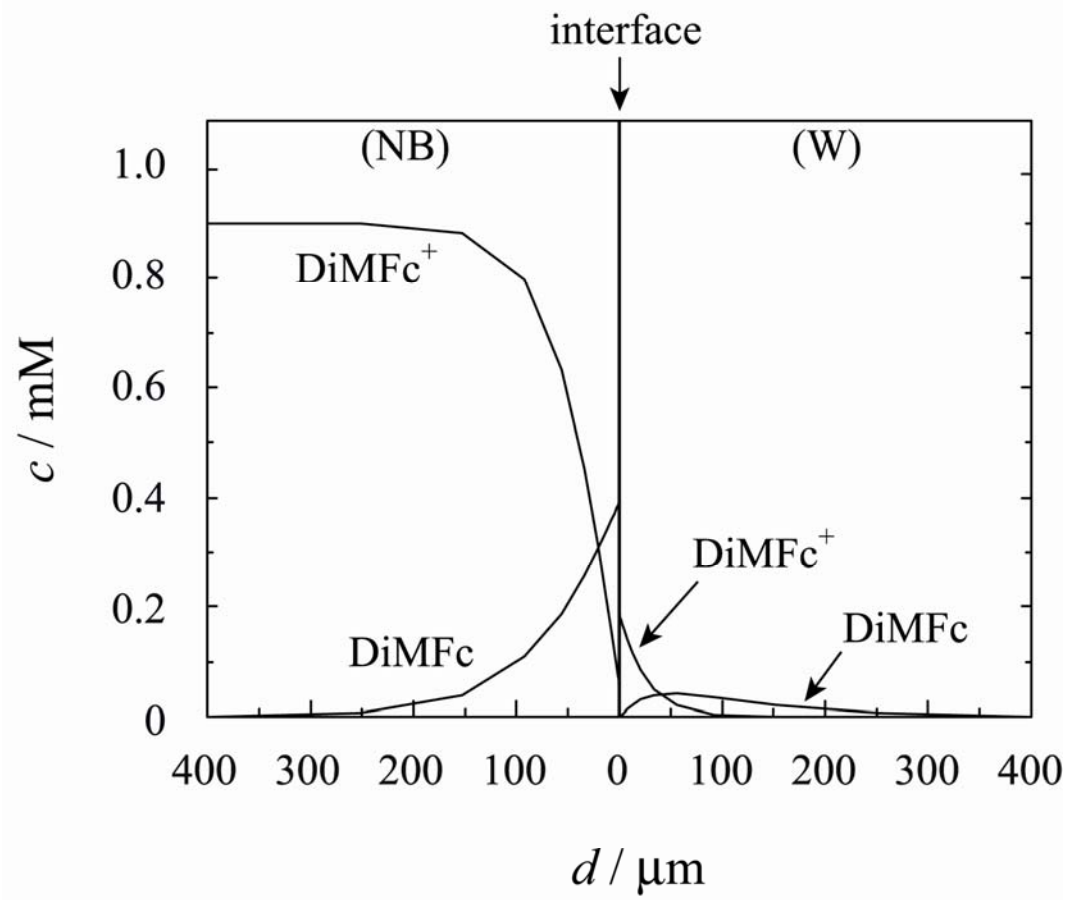
interface
(NB)
(W)
1.0
0.8
0.6
0.4
0.2
0
DiMFc+
DiMFc
DiMFc+
DiMFc
c / mM
400
300
200
100
0
100
200
300
400
d / μm

Fig. 6

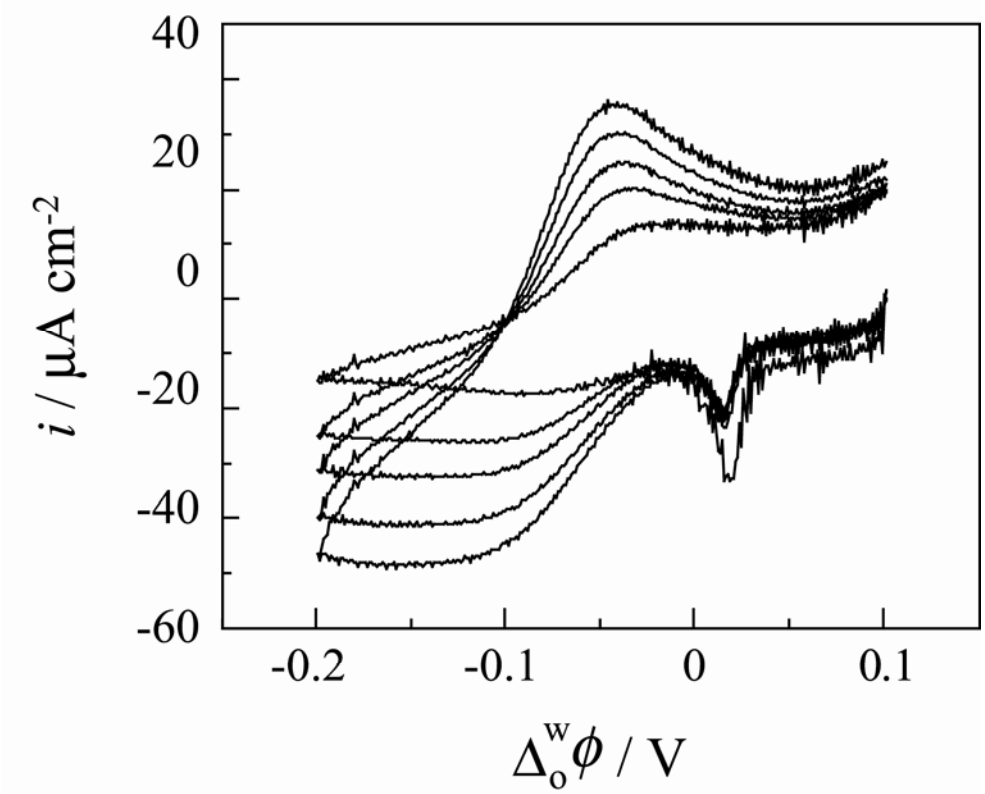

Fig. 7